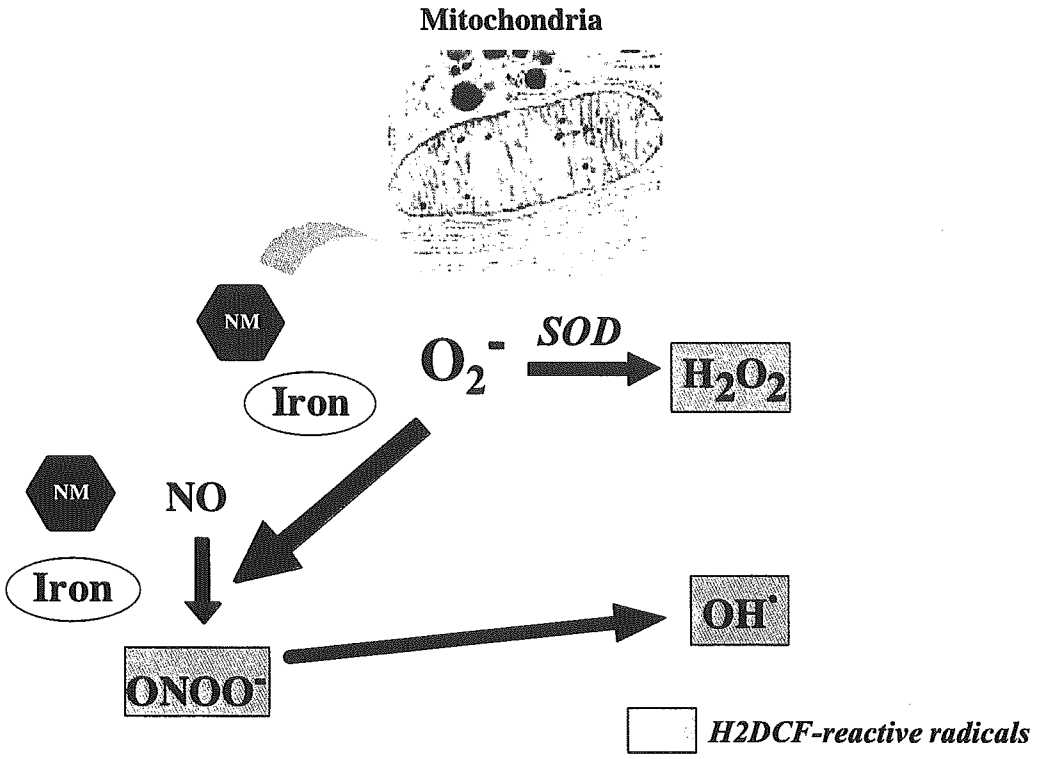

Fig. 5. The scheme how iron increases oxidative stress in mitochondria. Iron released from NM generates superoxide (O_2^-), which is catalized by SOD. O_2^- also reacts with nitric oxide (NO) by near-diffusion limit to produce peroxinitrite ($ONOO^-$). $ONOO^-$ is a strong radical itself and is decomposed into hydroxyl radical ($OH^\bullet$) also

reaction (Fig. 5). In the dopaminergic neurons, almost all the iron exists as bound with ferritin or NM, suggesting that NM may be neuroprotective, by chelating iron and other trace metals (Zecca et al., 2001b). Iron content in the substantia nigra increases by ageing but remained stable after the fourth decade of age, but NM content increases further according to ageing (Zecca et al., 2001a). In the postmortem PD brain, increased iron content was detected (Riederer et al., 1989) and recent results using transcranial ultrasonography revealed that in the substantia nigra of parkinsonian patients, not only the iron content increased, but that of NM decreased (Zecca et al., 2005). These results indicate that in the dopaminergic neurons in PD, the binding capacity of NM with iron was decreased and as a result, cytosolic free iron increased to inhibit ubiquitin-26S proteasome system, as shown in this paper (Gerlach et al., 2003).

Recent proteomics studies indicate the involvement of endosome-lysosome system as a source of proteinacious components in human NM (Tribl et al., 2005). This means NM production is not only "passive" accumulation of oxidative products, but some enzymatic system is required for the formation of high molecular aggregates. It requires further studies to elucidate whether the characteristics of NM itself or its synthetic pathway are changed in PD. The future studies on the intracellular mechanisms underlying the selective cell death by iron released by NM may bring out new strategies to prevent or rescue the decline in nigral dopamine neurons in PD.

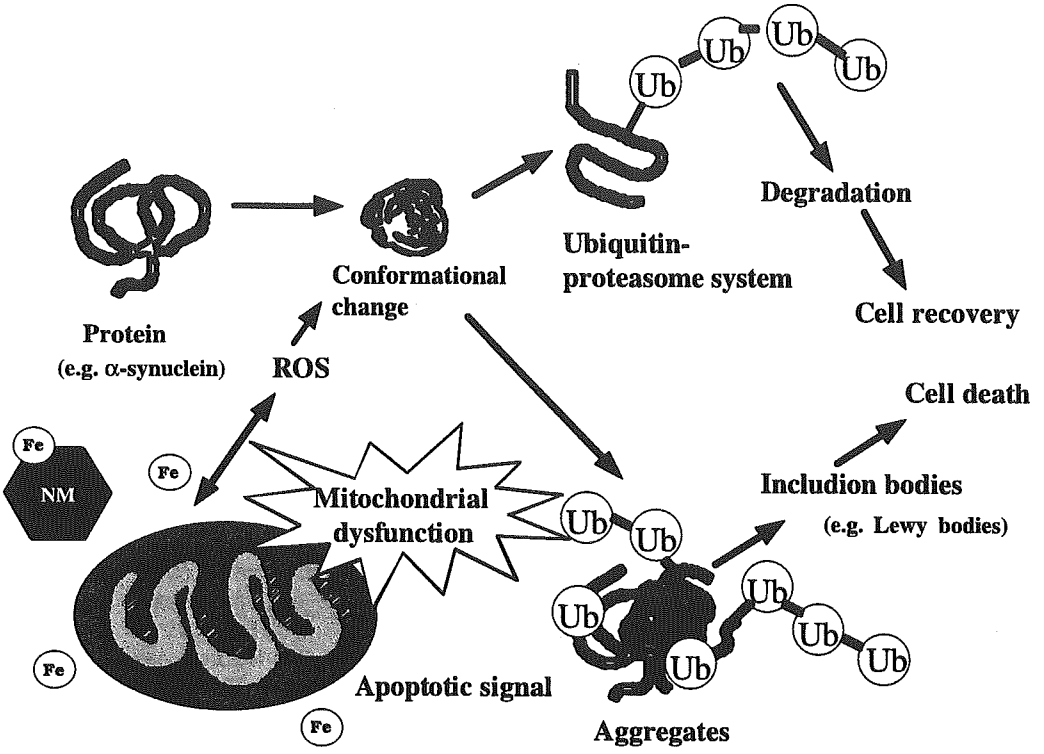

Fig. 6. The possible mechanism of dopaminergic neuronal death in Parkinson's disease. Iron released from NM increases oxidative stress in the mitochondria, and inhibit 26S proteasome system in the cells. Impairment of 26S proteasome increases accumulation of abnormal proteins to induce cell death ■

Acknowledgements

This work was supported by a Grant-in-Aid on Scientific Research for Young Scientists (B) for M. S. and (C) (W. M.) and (A) (W. M.) from Japan Society for the Promotion of Science, Grant for Research on Dementia and Bone Fracture (W. M., M. N.) from the Ministry of Health, Labor and Welfare, Japan.

References

Betarbet R, Sherer TB, MacKenzie G, Garcia-Osuna M, Panov AV, Greenamyre JT (2000) Chronic systemic pesticide exposure reproduces features of Parkinson's disease. Nat Neurosci 3: 1301–1306

Bradford MM (1976) A rapid and sensitive method for the quantitation of microgram quantities of protein using the principle of protein dye binding. Anal Biochem 72: 248–254

Crow JP (1997) Dichlorodihydrofluorescein and dihydrorhodamine 123 are sensitive indicators of peroxynitrite in vivo: Implications for intracellular measurement of reactive nitrogen and oxygen species. Nitric Oxide 1: 145–157

Desagher S, Osen-Sand A, Nichols A, Eskes R, Montessuit S, Lauper S, Maundrell K, Antonsson B, Martinou J-C (1999) Bid-induced conformational change of Bax is responsible for mitochondrial cytochrome c release during apoptosis. J Cell Biol 144: 891–901

Dexter DT, Sian J, Rose S, Hindmarsh JG, Mann VM, Cooper JM, Wells FR, Daniel SE, Lees AJ, Schapira AH (1994) Indices of oxidative stress and mitochondrial function in individuals with incidental Lewy body disease. Ann Neurol 35: 38–44

Double KL, Gerlach M, Schunemann V, Trautwein AX, Zecca L, Gallorini M, Youdim MB, Riederer P, Ben-Shachar D (2003) Iron-binding characteristics of neuromelanin of the human substantia nigra. Biochem Pharmacol 66: 489–494

Dzierzega-Lecznar A, Kurkiewicz S, Chodurek E, Stepien K, Wilczok T, Arzberger A, Riederer P, Gerlach M (2004) Neuromelanin of the human substantia nigra: structural investigations by pyrolysis-gas chromatography/mass spectrometry. J Am Soc Mass Spectrometry 15: 920–926

Faucheux BA, Martin ME, Beaumont C, Hauw JJ, Agid Y, Hirsch EC (2003) Neuromelanin asso-

ciated redox-active iron is increased in the substantia nigra of patients with Parkinson's disease. J Neurochem 86: 1142–1148

Fedorow H, Pickford R, Hook JM, Double KL, Halliday GM, Gerlach M, Riederer P, Garner B (2005) Dolichol is the major lipid component of human substantia nigra neuromelanin. J Neurochem 92: 990–995

Gerlach M, Trautwein AX, Zecca L, Youdim MB, Riederer P (1995) Mossbauer spectroscopic studies of purified human neuromelanin isolated from the substantia nigra. J Neurochem 65: 923–926

Jellinger K, Kienzl E, Rumpelmair G, Riederer P, Stachelberger H, Ben-Shacher D, Youdim MB (1992) Iron-melanin complex in substantia nigra of parkinsonian brains: an x-ray microanalysis. J Neurochem 59: 1168–1171

Kowall NW, Hantraye P, Brouillet E, Beal MF, McKee AC, Ferrante RJ (2000) MPTP induces alpha-synuclein aggregation in the substantia nigra of baboons. Neuroreport 11: 211–213

Leroy E, Boyer R, Auburger G, Leube B, Ulm G, Mezey E, Harta G, Brownstein MJ, Jonnalagada S, Chernova T, Dehejia A, Lavedan C, Gasser T, Steinbach PJ, Wilkinson KD, Polymeropoulos MH (1998) The ubiquitin pathway in Parkinson's disease. Nature 395: 451–445

McNaught KS, Jenner P (2001) Proteasomal function is impaired in substantia nigra in Parkinson's disease. Neurosci Lett 297: 191–194

Polymeropoulos MH, Lavedan C, Leroy E, Ide SE, Dehejia A, Dutra A, Pike B, Root H, Rubenstein J, Boyer R, Stenroos ES, Chandrasekharappa S, Athanassiadou A, Papapetropoulos T, Johnson WG, Lazzarini AM, Duvoisin RC, Di Iorio G, Golbe LI, Nussbaum RL (1997) Mutation in the alpha-synuclein gene identified in families with Parkinson's disease. Science 276: 2045–2047

Riederer P, Sofic E, Rausch WD, Schmidt B, Reynolds GP, Jellinger K, Youdim MB (1989) Transition metals, ferritin, glutathione, and ascorbic acid in parkinsonian brains. J Neurochem 52: 515–520

Shamoto-Nagai M, Maruyama W, Kato Y, Isobe K, Tanaka M, Naoi M, Osawa T (2003) An inhibitor of mitochondrial complex I, rotenone, inactivates proteasome by oxidative modification and induces aggregation of oxidized proteins in SH-SY5Y cells. J Neurosci Res 74: 589–597

Shamoto-Nagai M, Maruyama W, Akao Y, Osawa T, Tribl F, Gerlach M, Zucca FA, Zecca L, Riederer P, Naoi M (2004) Neuromelanin inhibits enzymatic activity of 26S proteasome in human dopaminergic SH-SY5Y cells. J Neural Transm 111: 1253–1265

Shimura H, Hattori N, Kubo S, Mizuno Y, Asakawa S, Minoshima S, Shimizu N, Iwai K, Chiba T, Tanaka K, Suzuki T (2000) Familiar Parkinson's disease gene product, parkin, is a ubiquitin-protein ligase. Nat Genet 25: 302–305

Tribl F, Gerlach M, Marcus K, Asan E, Tatschner T, Arzberger T, Meyer HE, Bringmann G, Riederer P (2005) "Subcellular Proteomics" of Neuromelanin Granules Isolated from the Human Brain. Mol Cell Proteomics 4: 945–957

Yoritaka A, Hattori N, Uchida K, Tanaka M, Stadtman ER, Mizuno Y (1996) Immunohistochemical detection of 4-hydroxynonenal protein adducts in Parkinson disease. Proc Natl Acad Sci USA 93: 2696–2701

Zecca L, Gallorini M, Schunemann V, Trautwein AX, Gerlach M, Riederer P, Vezzoni P, Tampellini D (2001a) Iron, neuromelanin and ferritin content in the substantia nigra of normal subjects at different ages: consequences for iron storage and neurodegenerative processes. J Neurochem 76: 1766–1773

Zecca L, Tampellini D, Gerlach M, Riederer P, Fariello RG, Sulzer D (2001b) Substantia nigra neuromelanin: structure, synthesis, and molecular behaviour. Mol Pathol 54: 414–418

Zecca L, Stroppolo A, Gatti A, Tampellini D, Toscani M, Gallorini M, Giaveri G, Arosio P, Santambrogio P, Fariello RG, Karatekin E, Kleinman MH, Turro N, Hornykiewicz O, Zucca FA (2004) The role of iron and copper molecules in the neuronal vulnerability of locus coeruleus and substantia nigra during aging. Proc Natl Acad Sci USA 101: 9843–9848

Zecca L, Berg D, Arzberger T, Ruprecht P, Rausch WD, Musicco M, Tampellini D, Riederer P, Gerlach M, Becker G (2005) In vivo detection of iron and neuromelanin by transcranial sonography: A new approach for early detection of substantia nigra damage. Mov Disord (in press)

Author's address: Dr. Wakako Maruyama, Department of Geriatric Medicine, National Center for Geriatrics and Gerontology, 36-3 Gengo, Morioka-cho, Obu, Aichi 474-8511, Japan, e-mail: maruyama@nils.go.jp

DOI 10.1007/s00702-005-0318-0
J Neural Transm (2006) 113: 125–135

Journal of Neural Transmission
Printed in Austria

Overexpression of amyloid precursor protein induces susceptibility to oxidative stress in human neuroblastoma SH-SY5Y cells

K. Matsumoto[1], Y. Akao[1], H. Yi[1], M. Shamoto-Nagai[2], W. Maruyama[2], and M. Naoi[1]

[1] Gifu International Institute of Biotechnology, Kakamigahara, Gifu, and
[2] Department of Geriatric Medicine, National Center for Geriatrics and Gerontology, Obu, Aichi, Japan

Received October 12, 2004; accepted April 9, 2005
Published online June 15, 2005;

Summary. In Alzheimer's disease amyloid β peptide (Aβ) produced from amyloid precursor protein (APP) is considered to induce cell death. To clarify the molecular mechanism underlying Aβ neurotoxicity, we established the cell line overexpressing wild or mutant (His684Arg) APP in human SH-SY5Y cells. This paper presents that overexpression of wild-APP in the cells (SH/w-APP) increased the levels of APP and $A\beta_{1-40}$ but not $A\beta_{1-42}$, and reduced Bcl-2 level and proteasome activity with increased susceptibility to oxidative stress. The intracellular levels of reactive oxygen species in SH/w-APP increased significantly by H_2O_2 treatment. The level of Bcl-2 protein, but not mRNA, was markedly decreased in SH/w-APP cells, which was inversely correlated with APP expression among subcloned SH/w-APP cells. These results indicate that increased expression of wild type APP renders neuronal cells more vulnerable to oxidative stress leading to cell death.

Keywords: Alzheimer's disease, amyloid precursor protein, apoptosis, oxidative stress, proteasome inhibitor, Bcl-2.

Abbreviations

AD Alzheimer's disease; *AMC* 7-amino-4-methyl-coumarin; *APP* β-amyloid precursor protein; $A\beta_{1-40}$ β-amyloid$_{1-40}$; $A\beta_{1-42}$ β-amyloid$_{1-42}$; *CM-H_2DCFDA* 5-(and-6)-chloromethyl-2,7-dichlorodihydrofluorescein diacetate; *BOC* *t*-butyloxycarbonyl; *DCF* 2′,7′-dichlorofluorescein; *FACS* fluorescence augmented flow cytometry; *GDNF* glial cell line-derived neurotrophic factor; *GSH* reduced glutathione; *PBS* phosphate-buffered saline; *PD* Parkinson's disease; *PT* permeability transition; *RNS* reactive nitrogen species; *ROS* reactive oxygen species; *RT* reverse transcription; *Z* benzyloxycarbonyl.

Introduction

In Alzheimer's disease (AD), abnormal protein–protein interactions may induce precipitation of protein, forming intracellular neurofibrillary tangles composed of hyperphosphorylated tau, and extracellular aggregates of senile plaques containing β-amyloid (Aβ) (Selkoe and Schenk, 2003). The major constituent of the core of senile plaques is

Aβ, a 39–43 amino acid peptide, produced from β-amyloid precursor protein (APP) by a series of proteases, β- and γ-secretases. Under normal conditions, APP is processed by a non-amyloidogenic pathway, where α-secretase produces soluble form of APP, whereas by an amyloidogenic pathway β- and γ-secretases generate Aβ with 40 or 42 amino acids in the length, β-amyloid$_{1-40}$ or $_{1-42}$ ($A\beta_{1-40}$, $A\beta_{1-42}$). The involvement of $A\beta_{1-40}$ and $A\beta_{1-42}$ in AD pathogenesis has been shown further by studies on mutations in *APP* gene causing early-onset autosomal-dominant AD. *APP* mutations increase the ratio $A\beta_{1-42}/A\beta_{1-40}$ (Miravelle et al., 2000), and $A\beta_{1-42}$ is prone to precipitation and aggregation constituting amyloid fibrils. This suggests that abnormal processing of APP and increase in Aβ may play a major role in the pathogenesis of the hereditary forms and also that of sporadic AD, since the pathological features of both forms of AD are almost the same. In addition, genetic variability in Aβ catabolism and cleavage was reported to contribute to the risk of late-onset AD (Wavrant-DeVrieze et al., 1999). The "amyloid hypothesis" (Hardy and Selkoe, 2002) elucidates most of the sequential pathological processes in AD; $A\beta_{1-42}$ deposition in plaques, activation of microglia and astrocytes, and dysfunction of synapse and neurons.

Recently in AD, apoptosis has been implicated as the potentially important mechanism underlying neuronal cell loss (Cotman and Anderson, 1995; Stadelmann et al., 1999). Aβ and presenilins 1 and 2 were found to drive cells into apoptosis (Loo et al., 1993). A number of hypotheses have been proposed to elucidate the mechanisms behind the induction of apoptosis by Aβ in AD; direct toxicity, such as increased oxidative stress, mitochondrial dysfunction, perturbed ionic homeostasis, and altered activities of kinases and phosphatases (Mattson et al., 1992; Behl et al., 1994; Ghosh et al., 1999; Avila, 2000). At the same time, Aβ increases vulnerability of neuronal cells to various insults including oxidative stress (Goodman et al., 1994). More recently, new mechanistic aspects for the cell death in AD have been gathering attention. Aβ activates the mitochondrial apoptotic cascade, through opening permeability transition pore (PTP), which Bcl-2 protein family regulates, either in an anti-apoptotic way (Bcl-2, Bcl-xL) or in a pro-apoptotic function (Bax, Bad) (Zhang et al., 2002). In addition, Aβ induces dysfunction in the proteasome system, which is responsible for the cellular proteolysis of most ubiquitinated, oxidized protein and regulates oxidative stress (Keller et al., 2000).

In this paper, the effects of increased synthesis of APP, and $A\beta_{1-40}$ and $A\beta_{1-42}$ were studied in concern to the morphological characteristics of the cells, the susceptibility to oxidative stress and proteasome inhibition. For the present study we established human SH-SY5Y cells overexpressing the wild and the mutated APP at the 684th amino acid from His to Arg, which is within $A\beta_{1-40}$ and $A\beta_{1-42}$ region. The results are discussed in relation to the interaction among cellular factors, anti-oxidant capacities and mitochondrial Bcl-2 levels, the reduction of which may lower threshold to cell death.

Materials and methods

Chemicals

Peroxynitrate-generating 3-(4-morpholinyl)sydonimine (SIN-1) was purchased from Dojindo (Kumamoto, Japan); geneticin from Invitrogen (San Diego, CA, USA); a proteasome inhibitor, benzyloxycarbonyl (Z)-L-isoleucyl-γ-*t*-butyl-L-glutamyl-L-alanyl-L-leucinol (PSI), 7-amino-4-methyl-coumarin (AMC), substrates for proteasome, *t*-butyloxycarbonyl (Boc)-Leu-Arg-Arg-MCA, Suc-Leu-Leu-Val-Tyr-MCA, and Z-Leu-Leu-Glu-MCA from Peptide Institute (Osaka, Japan). Hoechst 33342 and 5-(and-6)-chloromethyl-2,7-dichlorodihydrofluorescein diacetate (CM-H_2DCFDA) were purchased from Molecular Probes (Eugene, OR, USA). Hydrogen peroxide (H_2O_2) and other chemicals were purchased from Wako (Tokyo, Japan). SH-SY5Y cells were cultured in Cosmedium-001 tissue culture medium (CosmoBio, Tokyo, Japan) supplemented with fetal calf serum in an atmosphere of 95% air-5% CO_2

at 37°C. Antibodies were purchased as follows: anti-β-tubulin antibody from Sigma (St. Louis, Mo, USA), rabbit polyclonal anti-APP from Cell Signaling (Beverly, MA, USA), and mouse monoclonal anti-Bcl2, anti-Bcl-xL, and rabbit polyclonal anti-Bax from Santa Cruz Biotechnology (Santa Cruz, CA, USA).

Plasmid construction and DNA transfection of APP gene

Transfectants overexpressing wild APP were prepared with a pIRES1*neo* eukaryotic expression vector (Invitrogen, San Diego, CA, USA). For construction of pIRES1*neo-APP* vector, the coding region of human *APP* gene was obtained by reverse transcription (RT)-PCR from cDNA of SH-SY5Y cells and then inserted into the EcoRI-cleaved pIRES1*neo* vector. pIRES1*neo-APP* was confirmed to include wild-type *APP* gene by DNA sequencing. SH-SY5Y cells were transfected with pIRES1*neo* or pIRES1*neo-APP* by using liposomes (LipofectAMINE, GIBCO BRL, Rockville, MD, USA). The cells were selected using the culture medium containing 0.7 mg/ml geneticin (GIBCO BRL), and individual clones were isolated by limiting dilution, and characterized by RT-PCR and Western blot analysis. The stable clones overexpressing APP protein and control clone containing pIRES1*neo* vector were named as SH/w-APP and SH/IRES, respectively. The construction for an APP mutant, His684Arg, was performed by site-directed mutagenesis (BD Clontech, Franklin Lakes, NJ, USA) and the mutation was confirmed by DNA sequencing. The stable clone expressing APP mutant, His684Arg, was named as SH/m-684. In SH/w-APP cells, we further subcloned them by limiting dilution.

Quantitative real time RT-PCR

Total RNA was isolated using a Total RNA Extraction Kit (Amersham Biosciences, Piscataway, NJ, USA). RNA samples were reverse transcribed by Super Script II RNase H-reverse transcriptase (Invitrogen) using oligo(dT) primer (Invitrogen). Prepared cDNA samples were purified by a PCR Purification kit (QIAGEN, Hilden, Germany) and used for PCR.

Quantitative real time PCR was performed using a LightCycler Fast Start DNA Master SYBR Green I kit (Roche, Mannheim, Germany) in a LightCycler (Roche) according to the manufacturer's instruction. Primers for *APP* were as follows: *APP* forward, 5′-AAGAAGGCAGTTATCCAGCATTTC-3′; for *APP* reverse, 5′-TTGTAGAGCAGGGAGAGAGACTGA-3′. Primers for *Bcl-2* and *glyceraldehyde 3-phosphate dehydrogenase* (*GAPDH*) were commercially obtained from Roche. The PCR products were evaluated from the melting curve.

Quantitation of Aβ by the Sandwich ELISA

The culture medium of the cells cultured for 3 days was used for quantitative analyses of Aβ by the Sandwich ELISA for Aβ using Aβ ELISA kit (Biosource International, Camarillo, CA, USA). The values of Aβ concentrations in the medium were expressed as pg/ml. All ELISAs were carried out in duplicate.

Cell viability and morphological study

The vector-transfected SH-SY5Y cell clones grown in the presence of geneticin (G418, 0.7 mg/ml) were subjected to cell growth and morphological observation. Viable cell number was assessed by the trypan-blue dye exclusion test.

Immunocytochemistry

The cells were immunostained for β-tublin and F-actin as described in detail previously (Matsumoto et al., 2002). The cells were incubated with anti-β-tubulin antibody overnight at 4°C. After washing with PBS, the cells were incubated with the Alexa488-conjugated secondary antibody (Molecular Probes) for 1 h at room temperature. F-actin staining was performed with Alexa546-Phalloidin (Molecular Probes) for 30 min at room temperature. As negative control, we used the cells reacted with only the secondary antibody. The stained cells were observed with a fluorescence microscope, Olympus BX-51 (Olympus, Tokyo, Japan).

Detection of APP, Bcl-2, Bcl-xL and Bax by Western blotting analyses

Five micrograms of protein of each sample was analyzed for APP and Bcl-2 protein family, as previously described by Matsumoto et al. (2003). β-Tubulin was used as an internal control.

Measurements of production of reactive oxygen–nitrogen species by FACS

The production of reactive oxygen and nitrogen species (ROS-RNS) was quantitatively measured by the use of CM-H_2DCFDA, which detects H_2O_2, nitric oxide, and peroxynitrite. After treated with or without H_2O_2, the cells were washed twice with PBS, and CM-H_2DCFDA (10 μM in the final concentration) was added to the cell suspension in 25 mM HEPES, pH 7.5. After 30 min incubation at 37°C, the amount of 2′,7′-dichlorofluorescein (DCF) produced by CM-H_2DCFDA oxidation in the cell was determined by fluorescence-augmented flow cytometry (FACS) with a FACScaliber 4A and CellQuest software (Beckton Dickinson, San Jose, CA,

USA). The fluorometric measurement was performed with excitation at 488 nm and emission at 515–545 m.

Measurement of proteasome activity

The cells were suspended in the lysis buffer (50 mM Tris-HCl buffer, pH 7.75, 1 mM DTT, 0.5 mM EDTA and 5 mM $MgCl_2$) and incubated on ice for 30 min. The supernatants of centrifugation at 6000 g for 20 min were used as enzyme samples. Protein amount was measured with a DC Protein assay kit (Bio-Rad, Heoculos, CA, USA). Sample (10 μg protein) was incubated for 60 min at 37°C with MCA-conjugated substrates for three types of proteasome, Boc-Leu-

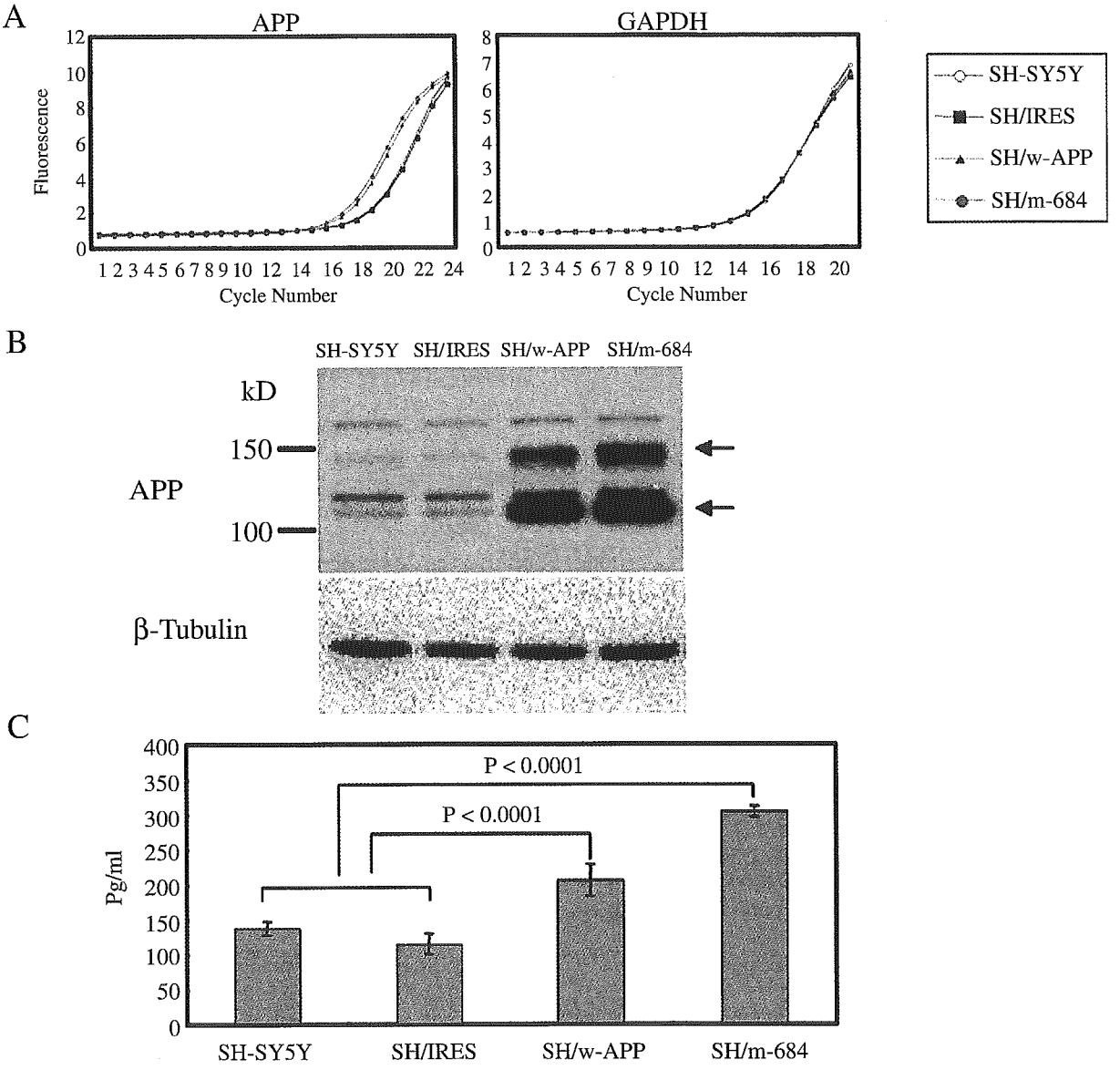

Fig. 1. Establishment of APP-overexpressing SH-SY5Y cells and assessment of the produced Aβ. **A** Real-time RT-PCR of *APP* and *GAPDH*. Cycle number and the fluorescent intensity corresponding to PCR product were shown. **B** Western blot analysis of APP. β-Tubulin was used as an internal standard. The arrows indicate the bands of APP. A band with the higher molecular weight corresponds to a modified APP probably by glycosylation and the lower one APP itself. **C** The amounts of $A\beta_{1-40}$ in the medium after 3 days' culture were assessed by ELISA. Difference from SH-SY5Y and SH/IRES is statistically significant

Arg-Arg-MCA for trypsin like, Suc-Leu-Leu-Val-Tyr-MCA for chymotrypsin like, and Z-Leu-Leu-Glu-MCA for postglutamyl peptidase-like activity. The released AMC fluorescence was measured in a fluoromicroplate reader, MTP-600 F (CORONA, Hitachinaka, Japan), with excitation at 380 nm and emission at 450 nm. The enzymatic activity was expressed as pmole/h/mg protein.

Measurement of intracellular GSH level

Intracellular reduced glutathione (GSH) content was quantitatively measured by using a GSH Assay Kit (Calbiochem, San Diego, CA). After cells were sonicated in 5% metaphosphoric acid and centrifuged at 3 000 g for 10 min, the supernatant was used to quantify GSH according to the manufacturer's instruction. The pellet dissolved in 1 M NaOH was used for the measurement of protein content. The GSH content was expressed as nmole/mg protein. Values were represented as the mean of three independent experiments.

Statistics

Differences were statistically evaluated by one way ANOVA followed by Fisher's PLSD. A p-value less than 0.05 was considered to be statistically significant.

Results

Establishment of APP-overexpressing SH-SY5Y cells

Real time RT-PCR study using *APP* specific P1 and P2 primers showed that the amounts of the products increased markedly in SH/w-APP transfected with wild APP, and SH/m-684 cells with mutated APP, compared to SH/IRES cells (Fig. 1A). The amount of APP protein of approximately 110 kDa and also modified form of APP with 140 kDa increased markedly in SH/w-APP and SH/m-684 cells, as determined by Western blot analysis (Fig. 1B). The amounts of $A\beta_{1-40}$ excreted in the culture medium are shown in Fig. 1C. $A\beta_{1-40}$ amounts significantly increased in SH/w-APP and SH/m-684 cells (Fig. 1C). The amount of $A\beta_{1-42}$ also increased in the culture medium of SH/m-684 cells to be 35 pg/ml, whereas it was under detection limit, 10 pg/ml, in that of other cell lines.

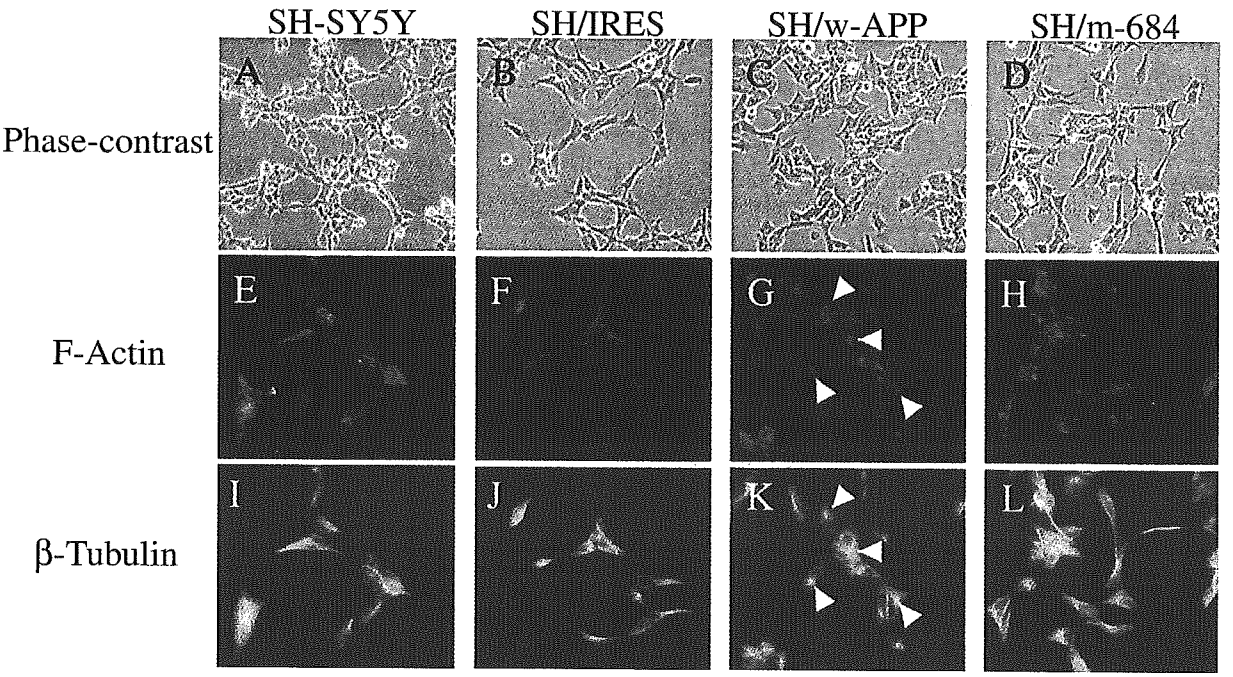

Fig. 2. Morphological study of the transfectants. *Upper panel*: phase-contrast aspects. *Middle and lower panel*: immunocytochemistry for F-Actin and β-Tubulin, respectively. The triangles indicate marked condensed regions of cytoskelton in SH/w-APP cells

Alteration of neurite net work formation in cells overexpressing wild-type APP

SH-SY5Y cells are usually sending out 1–2 long neurites, which contact with those of adjacent multiple cells forming a network with several cells. However, the morphological properties of SH/w-APP were markedly different from those of SH/IRES or SH/m-684 cells (Fig. 2A–D). SH/w-APP cells shaped polyhedral and had shorter and less branched neurites than other cell lines, which showed spindle form with neurites multi-directionally connected with adjacent cell bodies, as indicated in the staining of anti-F-actin and β-tubulin antibody (Fig. 2C).

Overexpression of wild APP sensitized the cells to oxidative stress, reduced proteasome activity, and increased GSH level

The effects of overexpression of wild and mutated APP on cell vulnerability were examined by exposing the cells to oxidative stress using H_2O_2, SIN-1 (a peroxynitrite donor), and PSI (an inhibitor of proteasome activity). The cells were treated with the agents for 12 h. The number of viable cells was shown in Fig. 3 and SH/w-APP was more sensitive to H_2O_2 than SH/IRES and SH/m-684. In addition, SIN-1and PSI also induced cell death more markedly in SH/w-APP than in other two cell lines.

The effects of APP overexpression on the ROS-RNS levels and the anti-oxidative capacity were examined by adding H_2O_2 to the culture medium. The intracellular ROS-RNS levels before and after H_2O_2 treatment were quantitatively determined as DCF produced from CM-H_2DCFDA (Fig. 4). The intracellular ROS-RNS levels of SH/w-APP cells significantly increased in a dose-dependent way (the middle panel), whereas in SH/IRES (the upper panel) and SH/m-684 cells (the lower panel) DCF levels were not affected by H_2O_2 (50 to 100 μM).

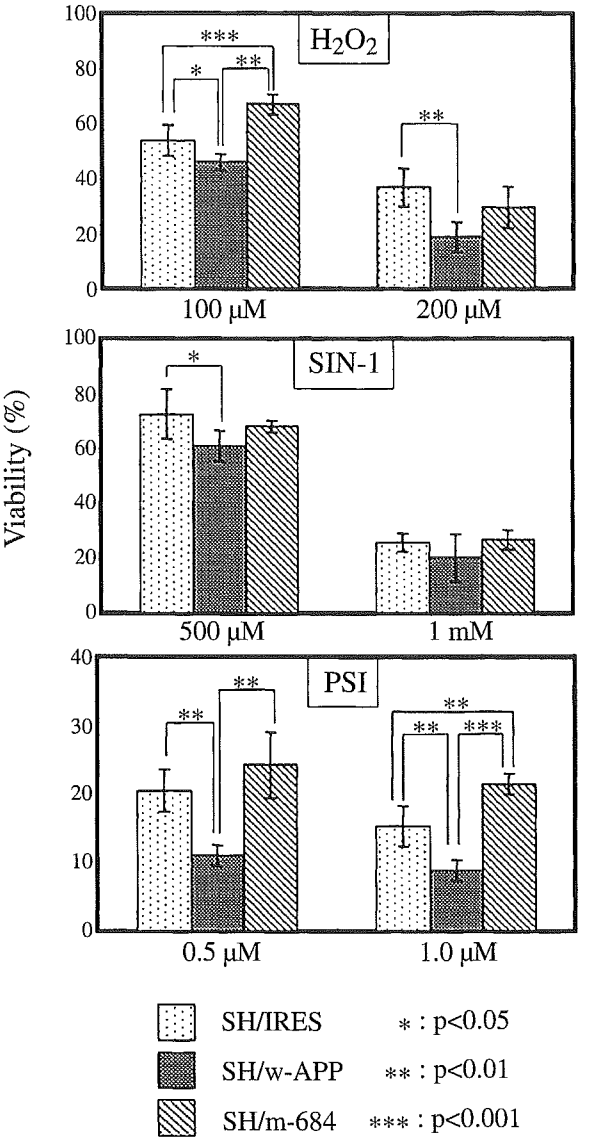

Fig. 3. The cell death induced y H_2O_2, SIN-1and PSI in the transfectants. Viable cell number was measured by trypan-blue dye exclusion test at 24 h after the treatment. *Upper panel*: Cells were treated with 100 and 200 μM H_2O_2. *Middle panel*: Treated with 500 μM and 1 mM SIN-1. *Lower panel*: Treated with 0.5 and 1 μM PSI. Data are expressed as means ± SD of four different experiments, and P values are evaluated by two-way ANOVA followed by Fisher's PLSD

The effect of APP overexpression on the activity of proteasome was examined in the cell lysate using synthetic fluorescent substrates without addition of ATP (Fig. 5). Trypsin-like activity of proteasome was significantly

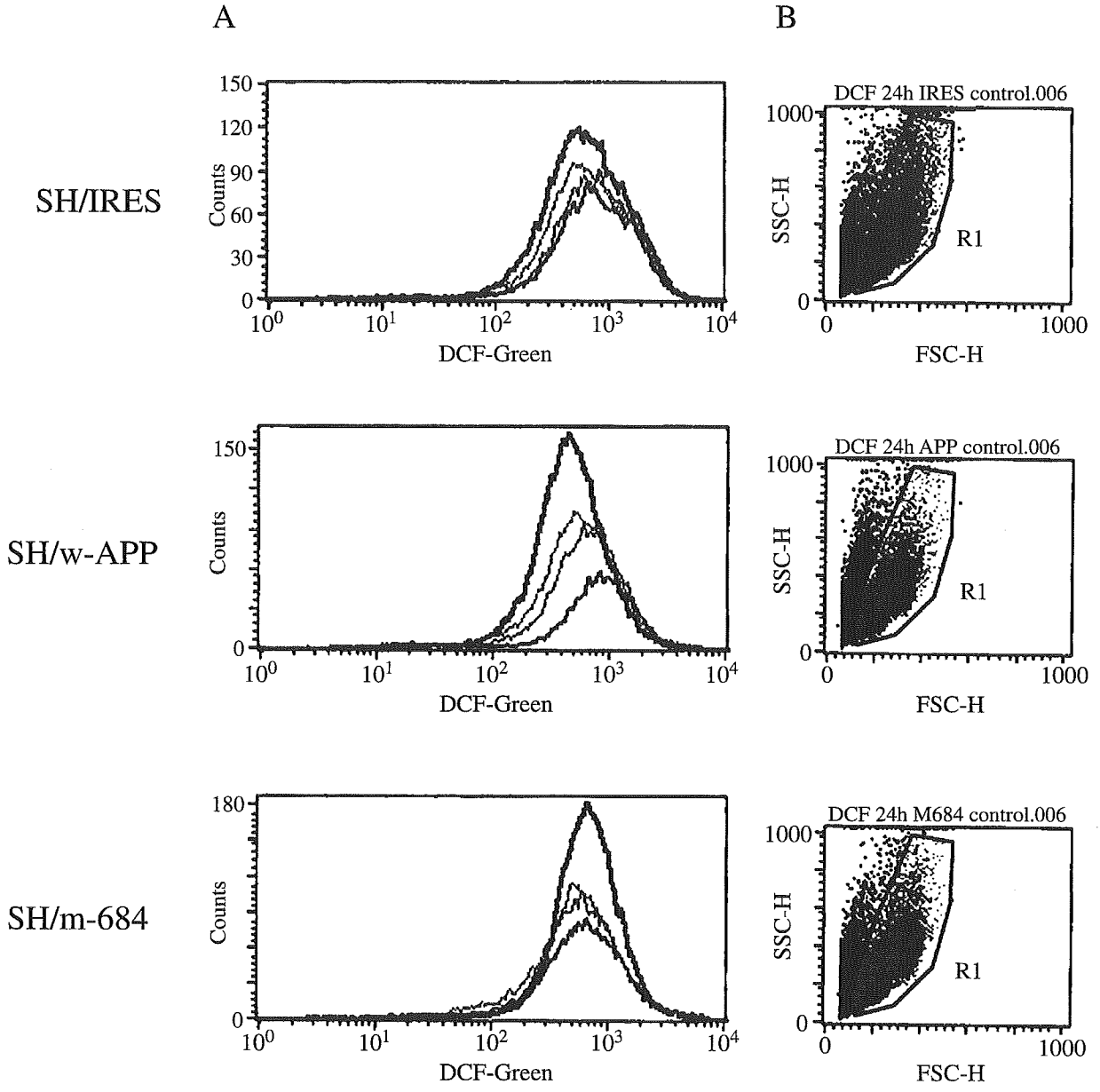

Fig. 4. The intracellular ROS-RNS levels after H_2O_2 treatment. The cells were treated with H_2O_2 for 24 h in serum-free medium. **A** The intracellular ROS-RNS levels measured by FACS using CM-H_2DCFDA. **B** Living cells were selected by FSC (forward scattered light)-H and SSC (side scattered light)-H (right panels)

reduced in SH/w-APP cells, whereas chymotrypsin-like and postglutamyl peptidase-like activities were only slightly reduced in SH/m-684 cells.

Moreover, as summarized in Table 1, the intracellular GSH levels were higher in SH/w-APP and SH/m-684 cells than control.

Effects of APP transfection on levels of Bcl-2 protein family

To clarify more detailed mechanism underlying oxidative stress-induced cell death, we examined the expression of Bcl-2 family protein regulating mitochondrial apoptotic mechanism in these transfectants. Among

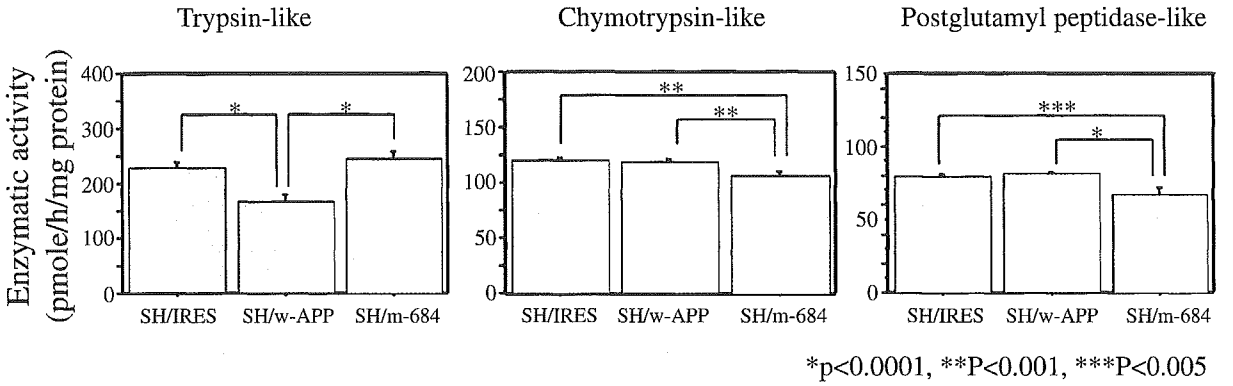

Fig. 5. The proteasome activity of the transfectants. The activities of trypsin-like, chymotrypsin-like and postglutamyl peptidase-like proteasome were quantified by use of respective fluorescent substrates. The column and bar represent the mean and SD of four independent experiments. Difference is statistically significant

the Bcl-2 family tested, only the level of Bcl-2 protein was decreased exclusively in SH/w-APP cells, whereas it did not change in other transfectants (Fig. 6A). On the other hand, the levels of Bcl-xL and Bax were not affected by the transfection of wild and mutated APP vectors. However, the level of *bcl-2* mRNA measured by the quantitative real time RT-PCR was almost same among the transfectants (Fig. 6B). The effects of APP overexpression on the modification of Bcl-2 protein were examined in SH/w-APP cells, but we could not detect any changes in amounts of phosphorylated form of Bcl-2 protein. In the subcloned cells of SH/w-APP cells, the levels of APP were inversely correlated with those of Bcl-2, as shown in Fig. 6C.

Discussion

In this paper, it was studied whether the excess synthesis of wild-type APP/Aβ or of $A\beta_{1-42}$ or $A\beta_{1-40}$ is truly toxic and involved in neuronal cells. In SH/w-APP cells with increased wild type APP and $A\beta_{1-40}$, formation of synaptic connections was impaired. Previously, we exposed SH-SY5Y cells to synthetic $A\beta_{1-42}$, but did not detect any morphological change or cell death, suggesting that increased *in situ* synthesis of APP itself may be responsible for such morphological changes. This finding may be relevant with the fact that the similar changes were detected in brains at the early stage of AD (Arendt, 2001).

In the brains from patients with AD, increased oxidative stress has been confirmed by detection of carbonyls (Smith et al., 1996), nitrated protein (Good et al., 1996; Smith et al., 1997), and protein adducts with lipid peroxidation endproducts (Sayre et al., 1997). Oxidative stress has been considered either as causes or consequences of Aβ production (Butterfield and Lauderback, 2002), and recently Aβ was reported to induce mitochondrial dysfunction through the conformational change in binding site with nicotinamide adenine dinucleotide, which may increase

Table 1. Intracellular levels of reduced glutathione in the transfectants

Transfectants	SH/IRES	SH/w-APP	SH/m-684
GSH content (nmole/mg protein)	20.05 ± 1.62	28.30 ± 1.73*	27.30 ± 1.56*

The number represents mean ± SD of 6 experiments. * $p < 0.01$ from SH/IRES

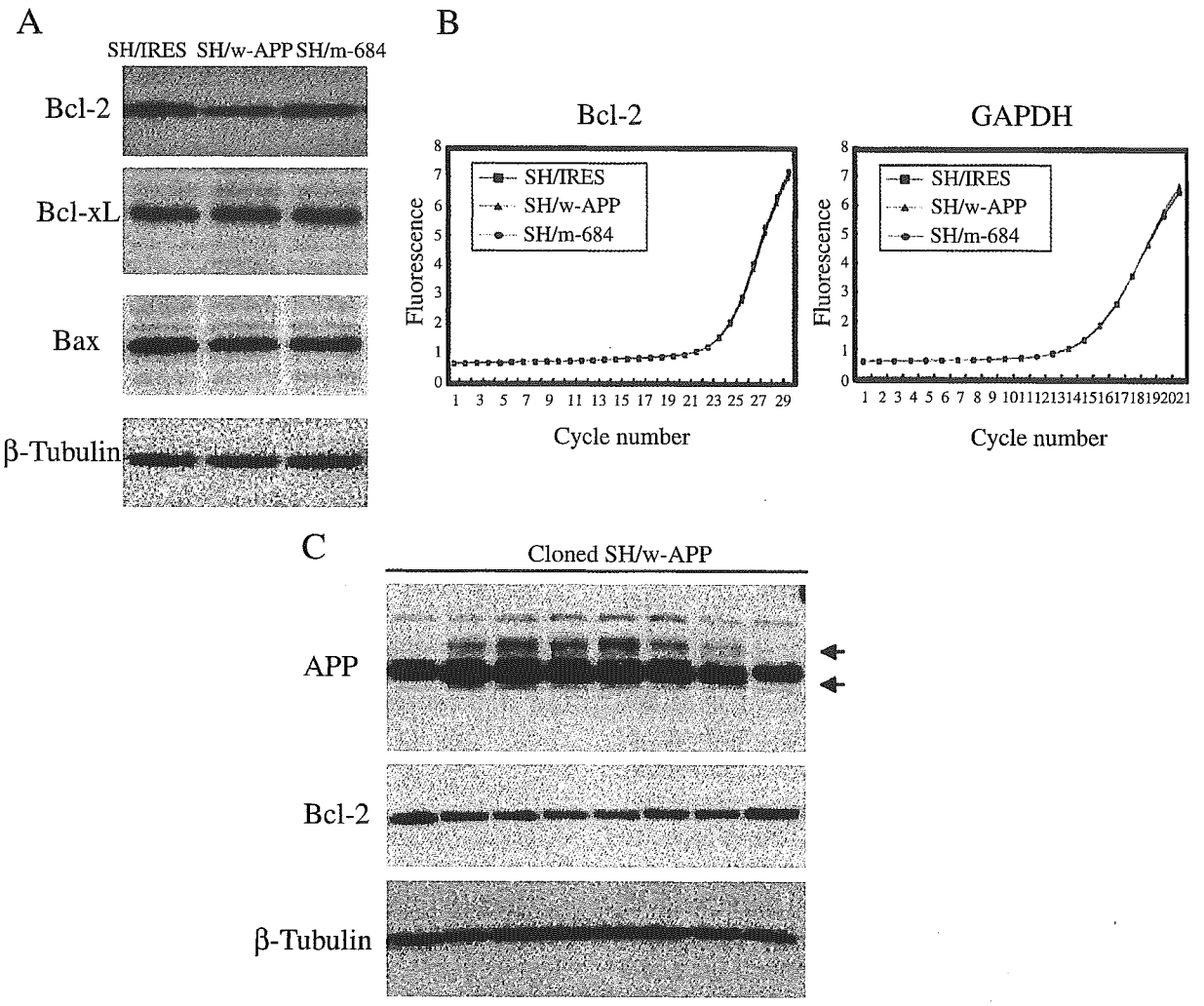

Fig. 6. The expression of apoptosis-related Bcl-2 family in the transfectants and the association of the expression between APP and Bcl-2 expression in SH/w-APP cells. **A** Western blot analysis of Bcl-2, Bcl-xL and Bax and β-tubulin used as an internal standard, in SH/IRES, SH/w-APP and SH/m-684 cells. **B** Real-time RT-PCR of *Bcl-2* and *GAPDH*. Cycle number and the fluorescent intensity corresponding to PCR product were shown. **C** Western blot analysis of APP, Bcl-2 and β-tubulin in subcloned cells overexpressing APP

oxidative stress (Lusbader et al., 2004). SH/w-APP cells overexpressing APP could survive and keep proliferation, and the level of ROS-RNS was not increased in steady state, even though anti-oxidative capacity was impaired, since H_2O_2 loading increased ROS-RNS and reduced the activity of proteasome, "the second scavenger" of ROS-RNS. Exposure to H_2O_2 or a proteasome inhibitor turned the compensating state in SH/w-APP cells into un-compensating state, further increased oxidative stress, and cell death was induced more markedly than in other transfectants.

The levels of anti-apoptotic Bcl-2 protein were reduced only in SH/w-APP, and the reduced levels were in an inverse correlation with the increased APP levels, which may be relevant with a previous report that Aβ peptides down-regulated Bcl-2 and upregulated Bax expression (Paradis et al., 1996). Selective reduction of Bcl-2 protein in SH/w-APP may be relevant with the increased sensitivity

to oxidative stress in this cell line. The ability of Bcl-2 to inhibit apoptosis induced by Aβ was reported to depend on its expression level (Ivins et al., 1999), supporting further our view. Anti-apoptotic Bcl-2 at sufficient concentrations regulates mitochondrial PT pore, and prevents apoptosis (Maruyama et al., 2002; Akao et al., 2003). It should be emphasized that not the mRNA level but the protein level of Bcl-2 was decreased in SH/w-APP cells. Since the phosphorylated Bcl-2 was not changed in our case, another posttranslational modification(s) may be involved in reduction of Bcl-2 protein. As a conclusion, only overexpression of wild type APP altered functional and morphological properties in the cells, while expression of mutated Aβ increased $A\beta_{1-42}$ excretion, but did not affect cell properties.

Mutations in APP, presenilin 1 and 2, and ApoE4 may increase ROS-RNS in neurons, but for a while the anti-oxidant system including the proteasome system can compensate enhanced oxidative stress. However, further insults, such as aging, other genetic or environmental factors, reduce anti-oxidant capacity further and lower the threshold to apoptosis. If we can control the increased oxidative stress and cell death using anti-oxidants (Gilgun-Sherki et al., 2003), or so-called neuroprotective agents, such as rasagiline, which induce the expression of pro-survival genes coding Bcl-2, Bcl-xL and neurotrophic factors (Akao et al., 2002; Maruyama et al., 2003, 2004; Weinstock et al., 2000), there will be a chance to protect neurons from cell death in AD. More work will be required for dissolving this problem.

Acknowledgements

This work was supported by a Grant-in-Aid for Scientific Research (Y. A., No. 09670859), on Scientific Research (C) (W. M.) and Center of Excellence Research Grant (Y. A.) from the Ministry of Education, Culture, Sports and Science and Technology, Japan, Grant-in-Aid for Scientific Research on Priority Areas (C) from Japan Society for the Promotion of Science (W. M.), Grant for Dementia and Bone Fracture (W. M., and M. N.) from the Ministry of Health, Labor and Welfare, Japan.

References

Akao Y, Maruyama W, Shimizu S, Yi H, Nakagawa Y, Shamoto-Nagai M, Youdim MBH, Tsujimoto Y, Naoi M (2003) Mitochondrial permeability transition mediates apoptosis induced by *N*-methyl(*R*)-salsolinol, an endogenous neurotoxin, and is inhibited by Bcl-2 and rasagiline, *N*-propargyl-1(*R*)-aminoindan. J Neurochem 82: 913–923

Arendt T (2001) Alzheimer's disease as a disorder of mechanisms underlying structural brain self-organization. Neuroscience 102: 723–765

Avila J (2000) Tau aggregation into fibrillar polymers: taupathies. FEBS Lett 476: 89–92

Behl C, Davis JB, Lesley R, Schubert D (1994) Hydrogen peroxide mediates amyloid β-protein toxicity. Cell 77: 817–827

Butterfield DA, Lauderback CM (2002) Lipid peroxidation and protein oxidation in Alzheimer's disease brain: potential causes and consequences involving β-peptide-associated free radical oxidative stress. Free Radic Biol Med 32: 1050–1060

Cotman CW, Anderson AJ (1995) A potential role of apoptosis in neurodegeneration and Alzheimer's disease. Mol Neurobiol 10: 19–45

Ghosh SS, Swerdlow RH, Miller SW, Sheeman B, Parker WD Jr, Davis RE (1999) Use of cytoplasmic hybrid cell lines for elucidating the role of mitochondrial dysfunction in Alzheimer's disease and Parkinson's disease. Ann NY Acad Sci 893: 171–191

Gilgun-Sherki Y, Melamed E, Offen D (2003) Antioxidant treatment in Alzheimer's disease. J Mol Neurosci 21: 1–11

Good PF, Werner P, Hsu A, Olanow CW, Perl DP (1996) Evidence for neuronal oxidative damage in Alzheimer's disease. Am J Pathol 149: 21–28

Goodman Y, Steiner MR, Steiner SM, Mattson MP (1994) Nordihydroguaiaretic acid protects hippocampal neurons against amyloid β-peptide toxicity and attenuates free radical and calcium accumulation. Brain Res 654: 171–176

Hardy J, Selkoe D (2002) The amyloid hypothesis of Alzheimer's disease; progress and problems on the road to therapeutics. Science 287: 353–356

Ivins KJ, Ivins JK, Sharp JP, Cotman CW (1999) Multiple pathways of apoptosis in PC12 cells. CrmA inhibits apoptosis induced by β-amyloid. J Biol Chem 274: 2107–2112

Keller JN, Hanni KB, Markesbery WR (2000) Impaired proteasome function in Alzheimer's disease. J Neurochem 75: 436–439

Loo DT, Copani A, Pike CJ, Whittemore ER, Walencewicz AJ, Cotman CW (1993) Apoptosis is induced by β-amyloid in cultured central nervous system neurons. Proc Natl Acad Sci USA 90: 7951–7955

Lustbader JW, Cirilli M, Lin C, Xu HW, Takuma K, Wang N, Casperen C, Chen X, Pollak S, Chaney M, Trinchese F, Liu S, Gunn-Moore F, Lue L-F, Walker DG, Kuppusamy P, Zewier ZL, Arancio O, Stern D, Yan SS, Wu H (2004) ABAD directly links Aβ to mitochondrial toxicity in Alzheimer's disease. Science 304: 448–452

Maruyama W, Akao Y, Youdim MBH, Davis BA, Naoi M (2001) Transfection-enforced Bcl-2 overexpression and an anti-Parkinson drug, rasagiline, prevent nuclear accumulation of glyceraldehydes-3-phosphate dehydrogenase induced by an endogenous dopaminergic neurotoxin, *N*-methyl(*R*)salsolinol. J Neurochem 78: 727–735

Maruyama W, Nitta A, Shamoto-Nagai M, Hirata Y, Akao Y, Youdim M, Furukawa S, Nabeshima T, Naoi M (2004) *N*-Propargyl-1(*R*)-aminoindan, rasagiline, increases glial cell line-derived neurotrophic factor (GDNF) in neuroblastoma SH-SY5Y cells through activation of NF-κB transcription factor. Neurochem Int 44: 393–400

Matsumoto K, Hiraiwa N, Yoshiki A, Ohnishi M, Kusakabe M (2002) Platelet-derived growth factor receptor-α deficiency in glomerular mesangial cells of tenascin-C knockout mice. Biochem Biophys Res Commun 290: 1220–1227

Matsumoto K, Akao Y, Kobayashi E, Ohguchi K, Ito T, Tanaka T, Iinuma M, Nozawa Y (2003) Induction of apoptosis by xanthones from Mangosteen in human leukemia cell lines. J Nat Prod 66: 1124–1127

Mattson MP, Cheng B, Davis D, Bryant K, Lieberburg I, Rydel RE (1992) β-Amyloid peptides destabilize calcium homeostasis and render human cortical neurons vulnerable to excitotoxicity. J Neurosci 12: 376–389

Miravalle L, Tokuda T, Chiarle R, Giaccone G, Burgiani O, Tagliavini F, Frangione B, Ghiso J (2000) Substitutions at codon 22 of Alzheimer's Aβ peptide induce diverse conformational changes and apoptotic effects in human cerebral endothelial cells. J Biol Chem 275: 27110–27116

Paradis E, Douillard H, Koutroumanis M, Goodyer C, LeBlanc A (1996) Amyloid β peptide of Alzheimer's disease downregulates Bcl-2 and upregulates Bax expression in human neurons. J Neurosci 16: 7533–7539

Sayre LM, Zelasko DA, Harris PLR, Perry G, Salomon RG, Smith MA (1997) 4-Hydrononenal-derived advanced lipid peroxidation end products are increased in Alzheimer's disease. J Neurochem 68: 2092–2097

Selkoe DJ, Schenk D (2003) Alzheimer's disease: molecular understanding predicts amyloid-based therapeutics. Annu Rev Pharmacol Toxicol 43: 545–584

Smith MA, Perry G, Richen PL, Sayre LM, Anderson VE, Beal MF, Kowall N (1996) Oxidative damage in Alzheimer's disease. Nature 382: 120–121

Smith MA, Harris PLR, Sayre LM, Beckman JS, Perry G (1997) Widespread peroxynitrite-mediated damage in Alzheimer's disease. J Neurosci 17: 2653–2657

Stadelmann C, Deckwerth TL, Srinivasan A, Bancher C, Brück W, Jellinger K, Lassmann H (1999) Activation of caspase-3 in single neurons and autophagic granules of granulovacuolar degeneration in Alzheimer's disease. Evidence for apoptotic cell death. Am J Pathol 155: 1459–1466

Wavrant-DeVrieze F, Lambert JC, Stas L, Crook R, Cottel D, Pasquier F, Frigard B, Lambrechts M, Thirty E, Amouyel P, Tur JP, Chartier-Harlin MC, Hardy J, Van Leuven F (1999) Association between coding variability in the LRP gene and the risk of late-onset Alzheimer's disease. Hum Genet 104: 432–434

Weinstock M, Goren T, Youdim MBH (2000) Development of a novel neuroprotective drug (TV3326) for the treatment of Alzheimer's disease, with cholinesterase and monoamine oxidase inhibitory activities. Drug Dev Res 50: 216–222

Zhang Y, McLaughlin R, Doodyer C, LeBlanc A (2002) Selective cytotoxicity of intracellular amyloid β peptide 1–42 through p53 and Bax in cultured primary human neurons. J Cell Biol 156: 519–529

Authors' address: Dr. Y. Akao, Gifu International Institute of Biotechnology, 1-1 Naka-fudogaoka, Kakamigahara, Gifu 504-0838, Japan, e-mail: yakao@giib.or.jp

DOI 10.1007/s00702-005-0299-z
J Neural Transm (2006) 113: 21–32

Journal of Neural Transmission
Printed in Austria

N-Propargylamine protects SH-SY5Y cells from apoptosis induced by an endogenous neurotoxin, *N*-methyl(*R*)salsolinol, through stabilization of mitochondrial membrane and induction of anti-apoptotic Bcl-2

H. Yi[1], W. Maruyama[2], Y. Akao[1], T. Takahashi[3], K. Iwasa[4], M. B. H. Youdim[5], and M. Naoi[1]

[1] Department of Neurosciences, Gifu International Institute of Biotechnology, Kakamigahara, Gifu,
[2] Department of Geriatric Medicine, National Center for Geriatrics and Gerontology, Obu, Aichi,
[3] Aichi-Konan College, Konan, Aichi, and
[4] Kobe Pharmaceutical University, Kobe, Japan
[5] Technion-Israel Institute of Technology, Faculty of Medicine, Eve Topf and NPF Centers, Haifa, Israel

Received January 10, 2005; accepted February 26, 2005
Published online April 22, 2005;

Summary. Propargylamine derivatives, rasagiline and (–)deprenyl, are anti-Parkinson agents and protect neurons from cell death as shown by *in vivo* and *in vitro* experiments. The studies on the chemical structure-activity relationship proved that the propargyl moiety is essentially required for the neuroprotective function. In this paper, neuroprotective activity of free *N*-propargylamine was studied using SH-SY5Y cells expressing only type A monoamine oxidase (MAO) against apoptosis induced by an endogenous dopaminergic neurotoxin, *N*-methyl(*R*)salsolinol. *N*-Propargylamine prevented apoptosis, whereas *N*-methylpropargylamine and propiolaldehyde did not. *N*-Propargylamine stabilized mitochondrial membrane potential and induced anti-apoptotic Bcl-2 at 1 μM–10 nM. *N*-Propargylamine inhibited MAO-A in competition to substrate with the apparent K_i value of 28 μM, which was significantly higher than the concentration required for neuroprotection. It indicates that MAO inhibition is not prerequisite for the protective function of *N*-propargylamine. The anti-apoptotic function of *N*-propargylamine is discussed in terms of neuroprotection by propargylamines in neurodegenerative diseases, including Parkinson's disease.

Keywords: Propargylamine, neuroprotection, apoptosis, mitochondrial membrane potential, Bcl-2, monoamine oxidase inhibitor.

Abbreviations

DMEM Dulbecco's modified Eagle's medium; *ERK* extracellular signal-regulated kinase; *FACS* fluorescence-augmented flow cytometry; *FCS* fetal calf serum; *2-HMP* *N*-(2-heptyl)-*N*-methylpropargylamine; *MAO*

monoamine oxidase; *MAO-A* and *MAO-B* type A and B MAO; *MAPK* mitogen-activated protein kinase; *NM(R)Sal N*-methyl(*R*)salsolinol [1(*R*),2(*N*)-dimethyl-6,7-dihydroxy-1,2,3,4-tetrahydroisoquinoline]; *PBS* phosphate-buffered saline; *PD* Parkinson's disease; *PI* propidium iodide; *PKC* protein kinase C; *PT* permeability transition.

Neuroprotection to delay or halt progressive degeneration of specified neurons is now proposed as a causal therapeutic strategy for Parkinson's disease (PD), Alzheimer's disease, and amyotrophic lateral sclerosis. In these disorders, apoptosis has been suggested to contribute to neuronal death, but this remains to be accepted in general. The well-regulated and slowly advancing process of apoptosis is proposed as a target of neuroprotection (Naoi and Maruyama, 2001; Vila and Przedborski, 2003). Various insults, including oxidative stress, metabolic compromise, excitotoxicity and endogenous and exogenous neurotoxins, are known to induce apoptosis in neurons. Apoptotic signaling is a multi-step pathway initiated by opening a mitochondrial mega-channel, called permeability transition (PT) pore, followed by decline in membrane potential ($\Delta\Psi$m), release of cytochrome c and other apoptosis-inducing factors, activation of caspases and final fragmentation of nuclear DNA. Mitochondrial PT and following apoptotic cascade are regulated by Bcl-2 protein family, and Bcl-2 and Bcl-xL prevent, and BAX and BAD promote cell death (Tsujimoto and Shimizu, 2000).

Recently, various candidates of neuroprotective agents have been proposed and some are now subjected for clinical trials (Ravina et al., 2003). A series of propargylamine derivatives, (–)deprenyl [selegiline, *N*-(phenylisopropyl)-*N*-methyl-propargylamine] (Riederer and Lachenmayer, 2003) and rasagiline [*N*-propargyl-1(*R*)-aminoindan] (Parkinson Study Group, 2002), were reported to have beneficial symptomatic effects in patients with PD. More recently clinical controlled study with rasagiline in Parkinsonian subjects was successfully carried out pointing to its possible action to modify or slow down the disease progress (Parkinson Study Group, 2004). The patients treated with rasagiline for 12 months showed less functional decline than those whose treatment was delayed for 6 months. *In vivo* and *in vitro* experiments confirmed that (–)deprenyl (Tatton et al., 1994; Maruyama and Naoi, 1999), rasagiline (Finberg et al., 1998; Maruyama et al., 2000, 2001a, 2002; Youdim et al., 2001b), and *N*-(2-heptyl)-*N*-methylpropargylamine [2-HMP] (Yu et al., 1994; Maruyama et al., 2001b) protect neuronal cells against apoptosis as induced by various insults. Significant insights into the anti-apoptotic function of propargylamine derivatives have been documented, and mitochondria emerge as a key organelle playing a regulatory role in apoptosis. Our previous studies have shown that the neuroprotection by propargylamine derivatives, specially rasagiline, is attributed to (1) the stabilization of $\Delta\Psi$m and prevention of PT (Maruyama et al., 2001a, b; Naoi et al., 2002a), (2) the induction of anti-apoptotic Bcl-2 family regulating PT (Akao et al., 2002a, b), (3) the release of glial cell line-derived neurotrophic factor (GDNF), a neurotrophic factor selective to dopamine neurons (Maruyama et al., 2004), and (4) activation of anti-oxidant enzymes, such as superoxide dismutase and catalase (Carrillo et al., 2000).

Most of the neuroprotective propargylamines, such as (–)deprenyl (Knoll et al., 1978) and rasagiline (Youdim et al., 2001a), are inhibitors of type B monoamine oxidase [monoamine, oxygen oxidoreductase (deaminating); EC 1.4.3.4; MAO-B], suggesting the involvement of MAO in the neuroprotective potency. (–)Deprenyl and 2-HMP (Yu et al., 1992) possess a methyl group at the nitrogen position of the propargylamine moiety and this gives them the potent MAO inhibitory activity (Yu et al., 1993). However, the desmethyl

metabolites of (–)deprenyl and 2-HMP, and (*S*)-enantiomer of rasagiline do not inhibit MAO-B, but protect neurons (Mytilineou et al., 1997; Maruyama et al., 2001c). These results suggest that the neuroprotective function of propargylamines may not depend on the MAO-inhibitory activity. On the other hand, the structure activity relationship of rasagiline analogues has indicated that *N*-propargylamine itself may stabilize $\Delta\Psi m$ and prevent apoptotic process (Maruyama et al., 2003). Indeed, free *N*-propargylamine was reported to protect PC12 cells from cell death induced by serum withdrawal (Weinreb et al., 2004) similar to rasagiline.

This paper describes the effects of *N*-propargylamine on apoptosis induced by a dopaminergic neurotoxin, *N*-methyl(*R*)salsolinol [1(*R*),2(*N*)-dimethyl-6,7-dihydroxy-1,2,3,4-tetrahydroisoquinoline, *N*M(*R*)Sal] (Maruyama et al., 1996, 2001b; Naoi et al., 2002b) in human dopaminergic neuroblastoma SH-SY5Y cells. Cell death induced by *N*M(*R*)Sal in SH-SY5Y cells has been confirmed to be apoptotic, not necrotic (Naoi et al., 2003), suggesting that this model may be adequate to examine the anti-apoptotic potency of *N*-propargylamine. The regulation of apoptotic signaling, namely stabilization of mitochondrial PT and expression of anti-apoptotic *bcl-2*, and effects on MAO activity by *N*-propargylamine were examined in SH-SY5Y cells, where only MAO-A activity is expressed. In addition, the structure-activity relationship in concern to anti-apoptotic function and MAO inhibiting potency were examined among *N*-propargylamine-related compounds, *N*-methylpropargylamine and propiolaldehyde.

Materials and methods

Materials

*N*M(*R*)Sal was prepared according to Teitel et al. (1972). Aminoindan was kindly supplied by TEVA Pharmaceutical Industries (Netanya, Israel). *N*-Propargylamine, kynuramine and 4-quinolinol were purchased from Sigma (St. Louis, MO, USA); *N*-methylpropargylamine from Aldrich (Milwaukee, WI, USA) and propiolaldehyde from Wako (Osaka, Japan); propidium iodide (PI), Mito-Tracker Orange and Green from Molecular Probes (Eugene, OR, USA), Dulbecco's modified Eagle's medium (DMEM) and other drugs from Nacalai tesque (Kyoto, Japan). SH-SY5Y cells were cultured in Cosmedium-001 tissue culture medium (CosmoBio, Tokyo, Japan), supplemented by 5% fetal calf serum (FCS) in an atmosphere of 95% air–5% CO_2. Mitochondria were prepared from SH-SY5Y cells according to Desagher et al. (1999).

Inhibition of MAO-A activity by N-propargylamine

MAO activity in mitochondria prepared from SH-SY5Y cells was measured fluorometrically according to the method reported by Kraml (1965) by use of kynuramine as a substrate. Kinetics for MAO activities and the inhibition by *N*-propargylamine were studied with 8 different concentrations of kynuramine. The values of the apparent Michaelis constant, K_m, and the apparent inhibitor constant, K_i, were calculated from the double-reciprocal plot of the reaction velocity against the substrate concentration. Protein concentration was determined according to Bradford (1976).

To determine the reversibility of the inhibition by *N*-propargylamine, MAO samples were incubated with 100 μM *N*-propargylamine for 30 min at 37°C, and then dialyzed against 10 mM sodium phosphate buffer, pH 7.4, at 4°C overnight. The MAO activities were quantified before and after the dialysis.

Assessment of apoptosis induced by NM(R)Sal

Apoptosis was quantitatively measured by fluorescence-augmented flow cytometry (FACS) with a FACScaliber 4A and CellQuest software (Becton Dickinson, San Jose, CA, USA). The cells cultured in a 6-well poly-L-lysine-coated culture flask were incubated in DMEM with or without 1 μM–1 nM *N*-propargylamine at 37°C for 30 min, then with 250 μM *N*M(*R*)Sal for 24 hr. The cells were treated with trypsin, gathered, washed with phosphate-buffered saline (PBS). To determine apoptotic cells, the cells were stained with 75 μM PI solution in PBS containing 1% Triton X-100 at room temperature for 5 min in the dark, washed and suspended in PBS, then subjected to FACS analysis. The fluorescence intensity at 560–640 nm (FL-2 channel) was detected for PI with excitation at 488 nm. To differentiate singlet from doublet cells, FL-2 (PI)-A (Area) and FL-2 (PI)-W (Width) parameters were used. Cells with a lower DNA content showing less PI staining than G1

were defined to be apoptotic cells (subG1 peak) (Eckert et al., 2001).

Measurement of ΔΨm in mitochondria isolated from SH-SY5Y cells

ΔΨm decline in isolated mitochondria by *N*M(*R*)Sal was quantitatively measured by FACS using MitoTracker Orange and Green. The mitochondria were suspended in DMEM and incubated with 10 μM *N*-propargylamine for 30 min at 37°C, then with 250 μM *N*M(*R*)Sal for 3 h. After stained with 100 nM MitoTracker Orange and Green for 30 min at 37°C, the mitochondria were washed and suspended with PBS and subjected to FACS. The laser emission at 560–640 nm (FL-2) and at shorter than 560 nm (FL-1) with excitation at 488 nm were used for the detection of MitoTracker Orange and Green fluorescence, respectively.

Determination of Bcl-2 protein levels in the cells treated with N-propargylamine

SH-SY5Y cells treated with 1 μM–1 pM *N*-propargylamine analogues for 24 h, and the cells were gathered, washed with PBS and suspended in RIPA buffer [10 mM Tris-HCl buffer, pH 7.5, containing 1% NP-40, 0.1% sodium deoxycholate, 0.1% sodium dodecyl sulfate, 150 mM NaCl and 1 mM EDTA 2Na]. The lyzed protein (5 μg) was separated by SDS-PAGE using 10–20% gradient polyacrylamide gel (Bio-Rad Lab., Hercules, CA, USA) and electroblotted onto PVDF membranes (Du Pont, Boston, MA, USA). After blockage with 5% nonfat milk in PBS containing 0.1% Tween 20, the membrane was incubated overnight at 4°C with anti-human Bcl-2 (100) antibody (Santa Cruz Biotechnology, Santa Cruz, CA, USA), or anti-tubulin

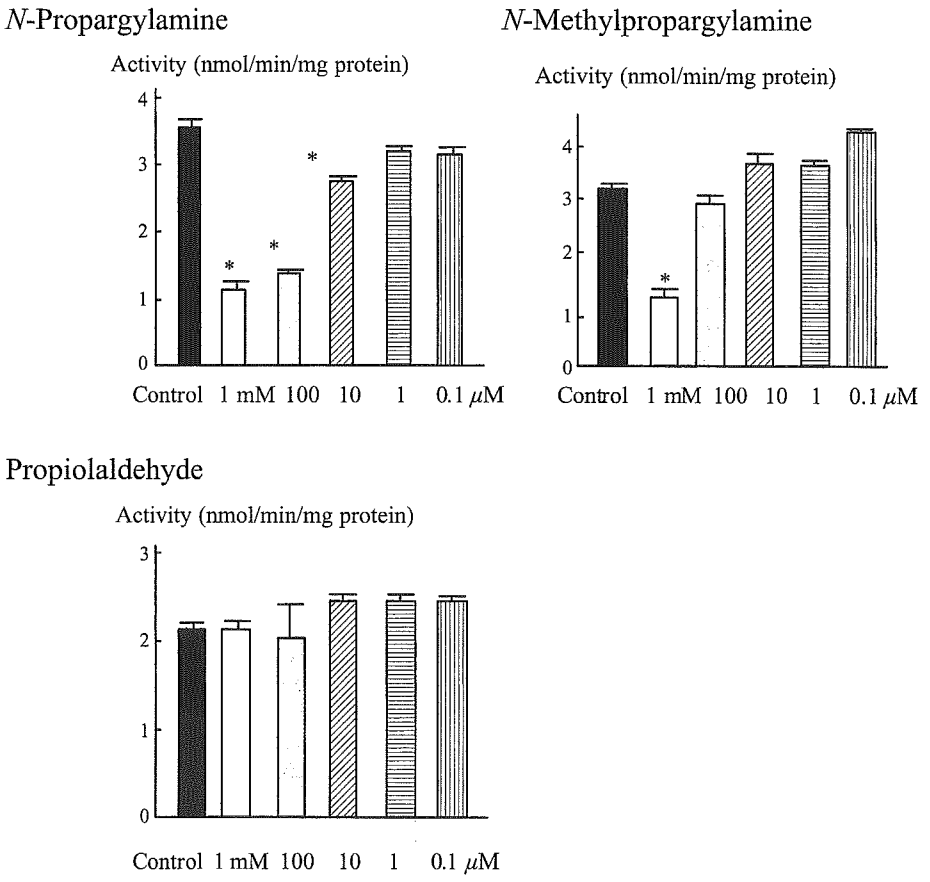

Fig. 1. The effects of *N*-propargylamine analogues on MAO-A activity. Mitochondria prepared from SH-SY5Y cells were used as MAO samples and incubated with 1 mM–0.1 μM *N*-propargylamine analogues and 100 μM kynuramine as a substrate at 37°C for 60 min, and the amounts of produced 4-hydroxyquinol were measured fluorometrically. The column and bar represent the mean and SD of 2 triplicate experiments. $P < 0.01$ from control

antibody as control (Sigma). The membranes were incubated further with alkaline phosphatase-conjugated goat anti-mouse antibody (Promega, Madison, WI, USA) at room temperature. The immunoblots were visualized by use of an enhanced chemiluminescence detection kit (New England Biolabs, Beverly, MA, USA).

Measurement of bcl-2 mRNA level in the cells treated with N-propargylamine

SH-SY5Y cells were cultured in the presence of various concentrations (1 μM–1 pM) of *N*-propargylamine for 24 h, and mRNA levels of *bcl-2* were quantitatively assessed by RT-PCR method (Akao et al., 2002a, b). The cells were gathered and washed with PBS, and the total RNA was extracted by the phenol/guanidinium thiocyanate method. cDNA was generated by reverse transcription of 2 μg of the total RNA, and the cDNA fragments were amplified using the PCR primers. The linearity of the amount of PCR product to the time of PCR amplification under the used conditions was confirmed by the real-time PCR method. PCR products were analyzed by electrophoresis on 3% agarose gels, and β-*actin* mRNA was used as an internal standard.

Statistics

Experiments were repeated at least 4 times in triplicate, and the results were expressed as the mean and SD. Differences were statistically evaluated by analysis of variance (ANOVA) followed by Sheffe's F-test. A p value less than 0.05 was considered to be statistically significant.

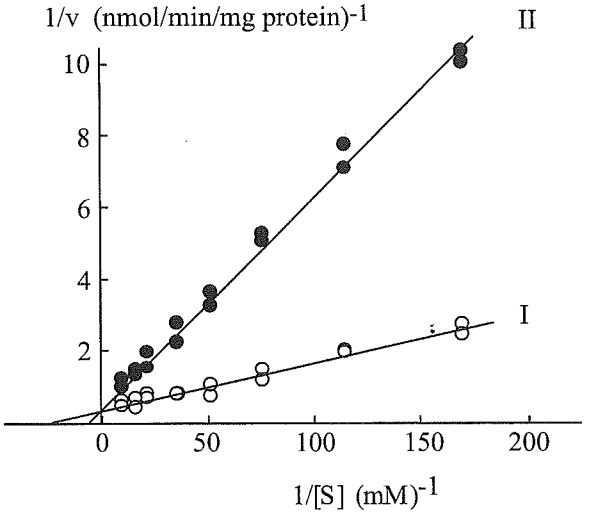

Fig. 2. The effects of *N*-propargylamine on the enzymatic activity of MAO-A. Mitochondria were prepared from SH-SY5Y cells, and MAO activity was measured fluorometrically with 8 different substrate concentrations in the absence (**I**) or presence of 100 μM *N*-propargylamine (**II**). The double reciprocal plots of the reaction velocity against the substrate concentration were used to calculate apparent K_m, K_i and V_{max} values, according the Lineweaver and Burk

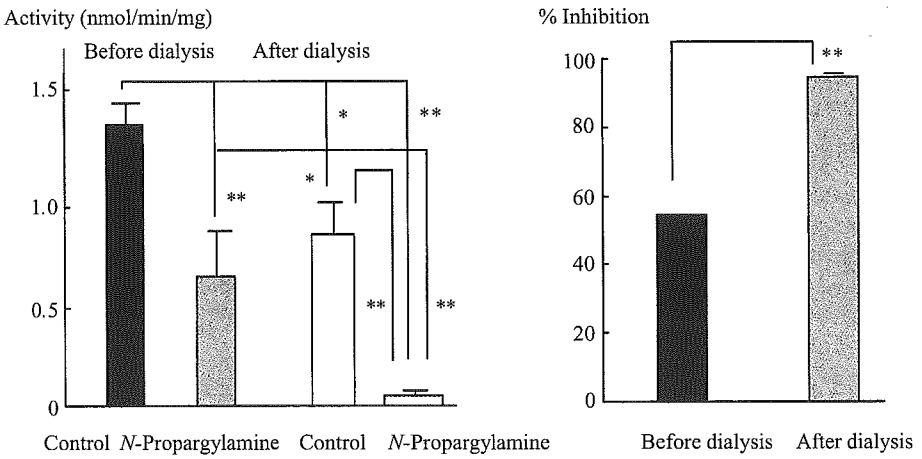

Fig. 3. Reversibility of MAO inhibition by *N*-propargylamine. MAO samples were treated with 100 μM *N*-propargylamine for 30 min at 37°C, then dialyzed against 10 mM sodium phosphate buffer, pH 7.4, at 4°C overnight. The MAO activity was measure with 100 μM kynuramine. The inhibition of MAO activity by *N*-propargylamine before and after dialysis was expressed as % inhibition by comparison of the reduced activity with the activity of control. $^*p<0.05$; $^{**}p<0.01$

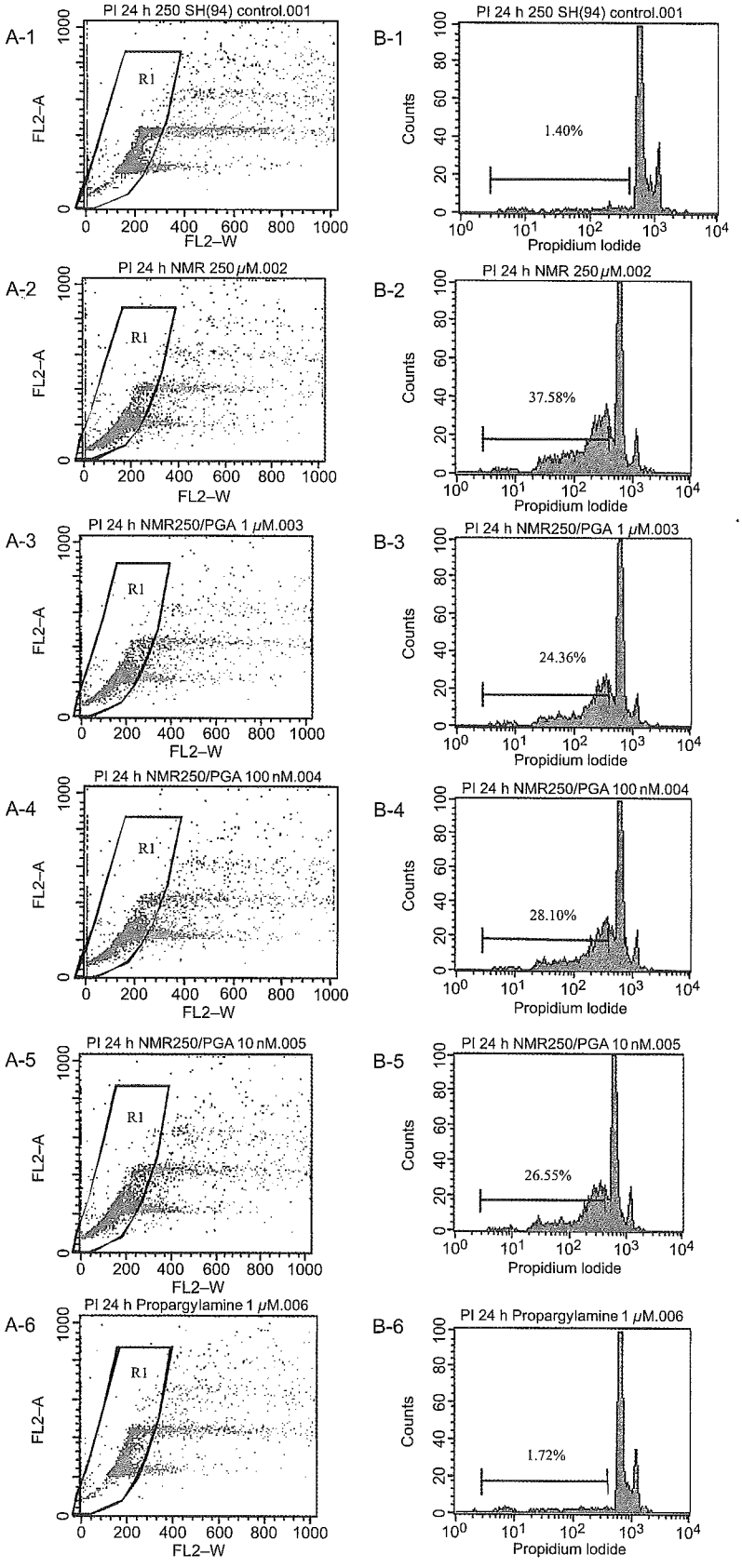
A-1
PI 24 h 250 SH(94) control.001
R1
FL2–A
FL2–W
B-1
PI 24 h 250 SH(94) control.001
1.40%
Counts
Propidium Iodide
A-2
PI 24 h NMR 250 μM.002
R1
FL2–A
FL2–W
B-2
PI 24 h NMR 250 μM.002
37.58%
Counts
Propidium Iodide
A-3
PI 24 h NMR250/PGA 1 μM.003
R1
FL2–A
FL2–W
B-3
PI 24 h NMR250/PGA 1 μM.003
24.36%
Counts
Propidium Iodide
A-4
PI 24 h NMR250/PGA 100 nM.004
R1
FL2–A
FL2–W
B-4
PI 24 h NMR250/PGA 100 nM.004
28.10%
Counts
Propidium Iodide
A-5
PI 24 h NMR250/PGA 10 nM.005
R1
FL2–A
FL2–W
B-5
PI 24 h NMR250/PGA 10 nM.005
26.55%
Counts
Propidium Iodide
A-6
PI 24 h Propargylamine 1 μM.006
R1
FL2–A
FL2–W
B-6
PI 24 h Propargylamine 1 μM.006
1.72%
Counts
Propidium Iodide